Applied Mathematical Biosystems, Volume 1, Issue 1, (Jul-Dec 2025), 1-9

Applied Mathematical Biosystems

journal homepage: https://ambjournal.com

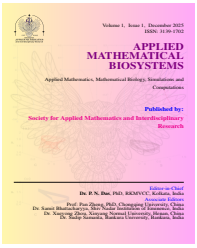

A mathematical model of cancer with delayed activation of immune cells

T. Pathak[1], **S. Paine**[1], **R. Kundu**[1], **S. Sarkar**[2], **S. Rana**[3] **and S. Samanta**[1]

[1]*Department of Mathematics, Bankura University, Bankura, West Bengal 722155, India*
[2]*Sri Aurobindo Vidyamandir, Chandannagar, Hooghly, West Bengal 712136, India*
[3]*Department of Mathematics, Indian Institute of Engineering Science and Technology, Shibpur, India*

Abstract

In this paper, we investigate a three-dimensional nonlinear cancer model describing the interactions among cancer cells, normal cells, and immune cells, incorporating a time delay to account for the delayed activation of the immune response. We first establish the biological feasibility of the model by proving the boundedness of its solutions. The equilibrium points of the system are determined, and their local stability is analyzed. Treating the time delay as a bifurcation parameter, we derive conditions for the occurrence of Hopf bifurcation, demonstrating that an increase in the delay can destabilize the system and induce oscillatory behavior. Numerical simulations are performed to validate the analytical findings and to illustrate rich dynamical phenomena, including limit cycle oscillations, period-doubling bifurcations, and chaotic dynamics. These results highlight the significant role of immune activation delay in shaping cancer dynamics.

Keywords: *Cancer model, Immune delay, Stability analysis, Bifurcation analysis, Chaos*

Corresponding author: Sudip Samanta *E-mail address:* samanta.sudip.09@gmail.com
Received: November 17, 2025 **Revised:** December 23, 2025 **Accepted:** December 23, 2025 **Published:** December 26, 2025
 DOI: 10.67029/j.amb.2025.0011.6

1. INTRODUCTION

Cancer is one of the most hazardous and life-threatening diseases worldwide and remains a major public health challenge [1]. It is a broad class of diseases characterized by uncontrolled growth of abnormal cells that can invade surrounding tissues and spread to distant organs. Cancer is the second leading cause of death globally after cardiovascular diseases, accounting for nearly one in six deaths each year. According to the International Agency for Research on Cancer (IARC), approximately 12.7 million new cancer cases and 7.6 million cancer-related deaths were reported worldwide in 2008. In 2020 alone, cancer caused nearly ten million deaths globally, with lung, breast, colorectal, prostate, stomach, and skin cancers being among the most prevalent types. This burden has continued to increase, with projections estimating 21.4 million new cases and 13.2 million deaths annually by 2030, primarily due to population growth, aging, and epidemiological transitions in developing countries [2].

Cancer treatment typically involves a combination of surgery, radiotherapy, chemotherapy, hormone therapy, and immunotherapy, with the choice of therapy depending on the cancer type, stage, and location. Early diagnosis remains crucial, as treatment outcomes are significantly improved when cancer is detected at an initial stage. Despite considerable advances in clinical oncology, cancer progression is governed by highly complex and nonlinear biological processes, including tumor growth, immune surveillance, angiogenesis, mutation, and interactions within the tumor microenvironment. Conventional therapies such as chemotherapy and ionizing radiation have long been employed to reduce tumor burden and, in some cases, achieve remission. However, tumor relapse frequently occurs due to the emergence of drug-resistant cancer cells, highlighting the limitations of monotherapy approaches and the need for more effective and targeted treatment strategies.

An appealing alternative and complementary approach to conventional therapies is immunotherapy, which aims to stimulate the body's immune system to recognize and eliminate cancer cells. The pioneering work of William Coley in the 1890s marked the earliest use of immunotherapy, employing bacterial toxins to induce anti-tumor immune responses [3]. More recently, cancer-preventive vaccines against hepatitis B virus and human papillomavirus have demonstrated remarkable success in reducing cancer incidence [4, 5]. In parallel, anti-angiogenic therapy, first proposed by Folkman [6], targets the tumor's blood supply by inhibiting angiogenesis, with vascular endothelial growth factor (VEGF) identified as a key regulator. Drugs such as bevacizumab have shown clinical efficacy, particularly when administered in combination with chemotherapy [7, 8, 9]. Nevertheless, these treatments may also affect healthy cells, and their overall effectiveness varies across cancer types.

The increasing complexity of therapeutic strategies has motivated the development of mathematical models as powerful tools for understanding cancer dynamics and optimizing treatment protocols. Mathematical modeling provides a

quantitative framework to integrate biological mechanisms, analyze tumor growth patterns, evaluate treatment responses, and design optimal therapy schedules. Several models have been proposed to study chemotherapy, immunotherapy, and anti-angiogenic treatments [10, 11, 12], although many neglect interactions with the tumor microenvironment or treatment-induced delays. Incorporating time delays into cancer models allows for a more realistic representation of biological latency and delayed immune or therapeutic responses [13]. Despite significant progress, accurate estimation of biological parameters from experimental or clinical data remains a major challenge. Consequently, the development of comprehensive mathematical models that integrate multiple treatment modalities and tumor–host interactions continues to be an active and essential area of research aimed at improving cancer management and patient outcomes.

Time delays are intrinsic to biological systems and arise from the finite time required for physiological, biochemical, and cellular processes to occur. In epidemiological modeling, incubation delays describe the latent period between pathogen exposure and the onset of infectiousness, whereas gestation delays represent the time lag between conception and birth, both of which play a fundamental role in shaping population dynamics [14, 15, 16, 17, 18, 19, 20, 21, 22]. Extensive studies on delayed predator–prey and multi-species systems further highlight the significance of delays in biological interactions; for instance, Beretta and Takeuchi examined the global stability of delayed Lotka–Volterra models with diffusion [23]. In medical and pharmacological settings, treatment or medication delays emerge due to delayed drug administration, absorption, distribution, and therapeutic response, significantly influencing disease control and treatment outcomes [24]. Additional delays arise from immune activation, cell differentiation, gene expression, and intracellular signaling pathways, introducing memory effects into biological systems and often leading to non-trivial dynamics [25]. In cancer modeling, time delays are particularly important for capturing tumor cell cycle durations, delayed immune surveillance, latency in angiogenesis, and postponed responses to chemotherapy or immunotherapy [13, 26, 27, 28]. Incorporating such delays into mathematical models frequently results in richer dynamics, including stability switches, oscillatory behavior, and Hopf bifurcations, thereby providing a more realistic description of biological processes and valuable insights into optimal therapeutic strategies [15, 25].

The inclusion of time delays can profoundly alter the dynamical behavior of cancer models, giving rise to complex phenomena such as sustained oscillations, bifurcations, multistability, and even deterministic chaos. These dynamical features may help explain irregular tumor growth, tumor recurrence, and multiple disease states observed in clinical practice. Time delays can destabilize an otherwise stable equilibrium or, conversely, stabilize an unstable system, thus playing a decisive role in determining long-term system behavior [1]. In the context of cancer modeling, Galach [29] introduced time delay into the Kuznetsov–Taylor cancer–immune interaction model [30] to better reflect biological realism [31]. These studies collectively demonstrate that time delays are not merely mathematical artifacts but essential components for accurately capturing the complexity of cancer dynamics.

In this present work, we study a three-dimensional cancer model with and without time delay. This paper is arranged as follows: In *Section 2*, we formulate a mathematical model on the basis of some biological assumptions and hypotheses. In *Section 3*, we provide general stability anlysis of the non-delayed model. Hopf bifurcation analysis has been carried out of the non-delayed system in *Section 4*. In *Section 5*, we modify our model introducing time-delay in the proliferation of immune cells and analyze the delayed cancer model. In *Section 6*, we perform numerical simulations of the non-delayed as well as delayed cancer model. Finally in *Section 7*, we briefly conclude with our main findings.

2. Cancer model

Here C, N, and I represent the populations of cancer cells, normal cells, and immune cells respectively at time t. The parameters r_1 and r_2 symbolized the growth rate of cancer cells and normal cells, respectively.

The model describes the interactions between cancer cells (C), normal cells (N), and immune cells (I), incorporating logistic growth and various interaction coefficients. Cancer cells grow logistically, but their growth is limited by competition with normal cells at rate a and destruction by immune cells at rate b. The normal cells also exhibit logistic growth, influenced by the presence of cancer cells, which activate their growth, while radiotherapy destroys them. The parameter d represents the rate at which normal cell decline due to influence of cancer cells. In this context, the term $\frac{eCI}{C+f}$ represents the activation and growth of immune system in response to the presence of cancer cells. Here, e denotes the maximum growth rate of effector cells and f is the half-saturation constant. And g represents the rate of inactivation of immune cells and h denotes the rate of mortality of immune cells.

Therefore, the model can be written as

$$\begin{aligned} \frac{dC}{dt} &= r_1C(1-C) - aCN - bCI, \\ \frac{dN}{dt} &= r_2N(1-N) - dCN, \\ \frac{dI}{dt} &= \frac{eCI}{C+f} - gCI - hI. \end{aligned} \tag{2.1}$$

The above model (2.1) has to be analyzed with the initial the condition $C(0) \geq 0$, $N(0) \geq 0$ and $I(0) \geq 0$.

2.1. Preliminary results

Boundness:

Theorem 2.1 *All the solutions of the above system (2.1) initiate in R^3_+ are uniformly bounded.*

Proof: Let us define $W(C, N, I) = C + N + I$.

The time derivative of W is

$$\begin{aligned} \frac{dW}{dt} &= \frac{dC}{dt} + \frac{dN}{dt} + \frac{dI}{dt} \\ &= r_1C(1-C) - aCN - bCI + r_2N(1-N) - dCN \\ &\quad + \tfrac{eCI}{C+f} - gCI - hI \\ &\leq r_1C - r_1C^2 + r_2N + r_2N^2 + eI - hI. \end{aligned} \tag{2.2}$$

Now,

$$\begin{aligned}\frac{dW}{dt}+\eta W &= r_1C-r_1C^2+\eta C+r_2N-r_2N^2+\eta N\\ &\quad +\eta I+(e-h)I\\ &= (r_1+\eta)C-r_1C^2+(r_2+\eta)N-r_2N^2\\ &\quad +\eta I+(e-h)I\\ &\le -r_1C^2+(r_1+\eta)C-r_2N^2+(r_2+\eta)N\\ &= -r_1\left(C-\frac{r_1+\eta}{2r_1}\right)^2+\frac{(r_1+\eta)^2}{4r_1}\\ &\quad -r_2\left(N-\frac{r_2+\eta}{2r_2}\right)^2+\frac{(r_2+\eta)^2}{4r_2}.\end{aligned}$$

Which implies

$$\frac{dW}{dt}+\eta W \le L, \tag{2.3}$$

where $L=L_1+L_2$ and $0<\eta<(h-e)$ with $L_1=\frac{(r_1+\eta)^2}{4r_1}$ and $L_2=\frac{(r_2+\eta)^2}{4r_2}$.

Applying the theory of differential inequality [32], we obtain

$$0<W(C,N,I)\le \frac{L}{\eta}+e^{-\eta t}\left[W(C(0),N(0),I(0))-\frac{L}{\eta}\right].$$

For $t\to\infty, 0<W(C,N,I)\le\frac{L}{\eta}$.

Hence we observe that the sum of three variables is bounded, which implies that each individual variable is bounded. Therefore, the entire system is bounded.

3. General stability analysis

3.1. Equilibrium points

The system (2.1) has five types of biologically feasible equilibrium points. The equilibrium points are given below:

(i) The trivial equilibrium point $E_0(0,0,0)$ always exists.
(ii)The axial equilibrium point $E_1(0,1,0)$ exists.
(iii)The axial equilibrium point $E_2(1,0,0)$ exists.
(iv)The planer equilibrium point $E_3(\bar{C},\bar{N},0)$, where

$$\begin{aligned}\bar{C} &= \frac{r_2(r_1-a)}{ad-r_1r_2},\\ \bar{N} &= \frac{r_1(d-r_2)}{ad-r_1r_2}.\end{aligned} \tag{3.1}$$

(v) The interior equilibrium point $E^*(C^*,N^*,I^*)$ where C^*,N^*,I^* are positive and satisfy the following relation

$$\begin{aligned}&r_1-r_1C^*-aN^*-bI^*=0,\\ &r_2-r_2N^*-dC^*=0,\\ &\frac{eC^*}{C^*+f}-gC^*-h=0.\end{aligned} \tag{3.2}$$

Solving the above system of equations (3.2) we obtain,

$$\begin{aligned}C^* &= \frac{-(fg+h-e)\pm\sqrt{(fg+h-e)^2-4fgh}}{2g},\\ N^* &= \frac{r_2-dC^*}{r_2},\\ I^* &= \frac{r_1-r_1C^*-aN^*}{b}.\end{aligned} \tag{3.3}$$

3.2. Local stability analysis

In this section, we investigate the local stability around the equilibrium points of the system (2.1) using the linearization technique. The Jacobian matrix of the any arbitrary equilibrium point (C,N,I) is

$$J(C,N,I)=\begin{bmatrix} a_{11} & -aC & -bC\\ -dN & a_{22} & 0\\ \frac{eIf}{(C+f)^2}-gI & 0 & \frac{eC}{C+f}-gC-h\end{bmatrix} \tag{3.4}$$

where $a_{11}=r_1-2Cr_1-aN-bI$ and $a_{22}=r_2-2Nr_2-dC$.

Theorem 3.1 *The equilibrium point $E_0(0,0,0)$ is always unstable.*

Proof: The eigenvalues of the Jacobian matrix around E_0 are $r_1,r_2,-h$. since $-h<0$, The trivial equilibrium point E_0 is stable if others two roots are negative i.e. $r_1<0$ and $r_2<0$. But the growth parameter r_1 and r_2 are always positive so the equilibrium point E_0 is unstable.

Theorem 3.2 *The equilibrium point $E_1(0,1,0)$ is a stable node if $r_1<a$ and $r_2>0$.*

Proof: The eigenvalues of the Jacobian matrix at $E_1(0,1,0)$ are $r_1-a, -r_2, -h$. So, E_1 will be stable if $r_1<a$ and $r_2>0$.

Theorem 3.3 *The equilibrium point $E_2(1,0,0)$ is a locally stable if $r_1>0, r_2>d$ and $\frac{e}{1+f}-g-h<0$.*

Proof: The eigenvalues of the Jacobian matrix evaluated at $E_2(1,0,0)$ are $-r_1, r_2-d, \frac{e}{1+f}-g-h$. So, E_2 will be locally stable if $r_1>0$ and $r_2>d$ and $\frac{e}{1+f}-g-h<0$.

Theorem 3.4 *The equilibrium point $E_3(\bar{C},\bar{N},0)$ is a locally stable if $\frac{e\bar{C}}{\bar{C}+f}-g\bar{C}-h<0$ and $r_1r_2>ad$.*

Proof: The Jacobian matrix around the equilibrium point E_3 is

$$J(E_3)=\begin{bmatrix} -r_1\bar{C} & -a\bar{C} & -b\bar{C}\\ -d\bar{N} & -r_2\bar{N} & 0\\ 0 & 0 & \frac{e\bar{C}}{\bar{C}+f}-g\bar{C}-h\end{bmatrix}.$$

The eigenvalues of the Jacobian matrix evaluated at $E_3(\bar{C},\bar{N},0)$ are $\frac{ec}{\bar{C}+f}-g\bar{C}-h$,

$$\frac{(-r_1\bar{C}-r_2\bar{N})\pm\sqrt{(-r_1\bar{C}-r_2\bar{N})^2-4(r_1r_2-ad)\bar{C}\bar{N}}}{2}.$$

Therefore, E_3 will stable if $\frac{e\bar{C}}{\bar{C}+f}-g\bar{C}-h<0$ and $r_1r_2>ad$.

Theorem 3.5 *The interior equilibrium point $E^*(C^*,N^*,I^*)$ is locally asymptotically stable if $\psi_1>0,\psi_2>0,\psi_3>0$ and $\psi_1\psi_2>\psi_3$.*

Proof: The Jacobian matrix around the equilibrium point E^* is

$$J(E^*)=\begin{bmatrix} -r_1C^* & -aC^* & -bC^*\\ -dN^* & -r_2N^* & 0\\ \frac{eI^*f}{(C^*+f)^2}-gI^* & 0 & 0\end{bmatrix}.$$

The characteristic equation of the above matrix around the interior equilibrium point $E^*(C^*,N^*,I^*)$ is given by

$$\xi^3+\psi_1\xi^2+\psi_2\xi+\psi_3=0, \tag{3.5}$$

where

$$\psi_1 = (r_1C^* + r_2N^*),$$
$$\psi_2 = r_1r_2C^*N^* - adC^*N^* + bC^*\left(\frac{efI^*}{(C^*+f)^2} - gI^*\right),$$
$$\psi_3 = br_2C^*N^*\left(\frac{efI^*}{(C^*+f)^2} - gI^*\right).$$

Therefore, the interior equilibrium point $E^*(C^*, N^*, I^*)$ will be locally stable if the coefficients of the characteristic equation satisfies the the Routh-Hurwitz stability criterion *i.e.* if $\psi_1 > 0, \psi_2 > 0, \psi_3 > 0$ and $\psi_1\psi_2 > \psi_3$.

4. Hopf bifurcation analysis

Theorem 4.1 *The system (2.1) undergoes a Hopf-bifurcation around the positive interior equilibrium when the maximum growth rate of effector cells e exceeds a critical value. The Hopf bifurcation occurs at $e = e^*$ if and only if the following condition holds*
(i) $H_b(e^*) \equiv \psi_1(e^*)\psi_2(e^*) - \psi_3(e^*) = 0$,
(ii) $\frac{d}{de}[Re(\xi(e))]_{e=e^*} \neq 0$,
where ξ is the root of characteristic equation (3.5).

Proof: Let $e = e^*$, then the characteristic equation (3.5) transforms to

$$(\xi^2 + \psi_2)(\xi + \psi_1). \tag{4.1}$$

Clearly, the roots of the equation (4.1) are $\xi_1 = i\sqrt{\psi_2}$, $\xi_2 = i\sqrt{\psi_2}$, $\xi_3 = -\psi_1$. Now we can rewrite the roots considering e as bifurcation parameter as follows

$$\begin{aligned} \xi_1(e) &= \phi_1(e) + i\phi_2(e), \\ \xi_2(e) &= \phi_1(e) - i\phi_2(e), \\ \xi_3(e) &= -\psi_1(e). \end{aligned} \tag{4.2}$$

Substituting $\xi_1(e) = \phi_1(e) + i\phi_2(e)$ into (3.5) and differentiating with respect to e , and then separating the real and imaginary parts, we obtain

$$\begin{aligned} X(e)\phi_1'(e) - Y(e)\phi_2'(e) + U(e) = 0, \\ Y(e)\phi_1'(e) + X(e)\phi_2'(e) + V(e) = 0, \end{aligned} \tag{4.3}$$

where

$$\begin{aligned} X(e) &= 3\phi_1^2(e) + 2\psi_1(e)\phi_1(e) + \psi_2(e) - 3\phi_2^2(e), \\ Y(e) &= 6\phi_1(e)\phi_2(e) + 2\psi_1(e)\phi_2(e), \\ U(e) &= \phi_1^2(e)\psi_1'(e) + \psi_2'(e)\phi_1(e) + \psi_3'(e) - \psi_1'(e)\phi_2^2(e), \\ V(e) &= 2\phi_1(e)\phi_2(e)\psi_1'(e) + \psi_2'(e)\phi_2(e). \end{aligned} \tag{4.4}$$

At $e = e^*$, we have $\phi_1(e^*) = 0$ and $\phi_2(e^*) = \sqrt{\psi_2(e^*)}$.
Using these results, we get
$X(e^*) = -2\psi_2(e^*)$,
$Y(e^*) = 2\psi_1(e^*)\sqrt{\psi_2(e^*)}$,
$U(e^*) = \psi_3'(e^*) - \psi_1'(e^*)\psi_2(e^*)$,
$V(e^*) = \psi_2'(e^*)\sqrt{\psi_2(e^*)}$.
Now,

$$\frac{d}{de}[Re(\xi(e))]_{e=e^*} = \frac{Y(e^*)V(e^*) + X(e^*)U(e^*)}{X(e^*)^2 + Y(e^*)^2}$$
$$= \frac{\psi_1(e^*)\psi_2'(e^*) - \psi_3'(e^*) + \psi_1'(e^*)\psi_2'(e^*)}{2(\psi_2(\lambda^*)) + (\psi_1(\lambda^*))^2}$$
$\neq 0$, if $\psi_1(e^*)\psi_2'(e^*) - \psi_3'(e^*) + \psi_1'(e^*)\psi_2(e^*) \neq 0$
and $\xi_3(e^*) = -\psi_1(e^*) \neq 0$.

So, the transversality condition (*i.e.* condition (ii)) holds and the system (2.1) exhibits Hopf bifurcation at $e = e^*$.

5. Cancer Model with delay

To account for the delay in proliferation of the immune cells, we revise the model (2.1) accordingly by incorporating a time-delay ($\tau > 0$) in the immune cells, and then model (2.1) takes the modified form as:

$$\begin{aligned} \frac{dC}{dt} &= r_1C(1-C) - aCN - bCI, \\ \frac{dN}{dt} &= r_2N(1-N) - dCN, \\ \frac{dI}{dt} &= \frac{eC(t-\tau)I(t-\tau)}{C(t-\tau)+f} - gCI - hI. \end{aligned} \tag{5.1}$$

For analysing system (5.1), we take the initial condition as follows:

$$C(\theta) = \psi_1(\theta), N(\theta) = \psi_2(\theta), I(\theta) = \psi_3(\theta), -\tau \leq \theta \leq 0, \tag{5.2}$$

where $\psi = (\psi_1, \psi_2, \psi_3) \in \mathbb{C}_+$ such that $\psi_i(\theta) \geq 0, i = 1, 2, 3 \ \forall \ \theta \in [-\tau, 0]$ and $\mathbb{C}_+$ denotes Banach space $\mathbb{C}_+([-\tau, 0], \mathbb{R}^3_{0,+})$ of continuous functions mapping the interval $[-\tau, 0]$ into $\mathbb{R}^3_{0,+}$. We define the norm of an element ψ in $\mathbb{C}_+$ by $||\psi|| = \sup_{-\tau\leq\theta\leq 0}\{|\psi_1(\theta)|, |\psi_2(\theta)|, |\psi_3(\theta)|\}$. Moreover, we assume that $\psi_i(0) \geq 0$ for each i. The fundamental theory of functional differential equations [33] ensures that there exists a unique solution $C(t), N(t), I(t)$ to the delayed system (5.1) with initial conditions (5.2).

5.1. Stability and bifurcation analysis

5.1.1. Characteristic equation

Let $E^*(C^*, N^*, I^*)$ be any arbitrary equilibrium point. The Jacobian matrix around E^* leads us to the following characteristic equation

$$det(J_0 + e^{-\lambda\tau}J_\tau - \lambda I_3) = 0, \tag{5.3}$$

where I_3 is the identity matrix of order 3 and

$$J_0 = \begin{pmatrix} V_1 & -V_2 & -V_3 \\ V_4 & V_5 & 0 \\ V_6 & 0 & -V_7 \end{pmatrix},$$

and

$$J_\tau = \begin{pmatrix} 0 & 0 & 0 \\ 0 & 0 & 0 \\ M_1 & 0 & M_2 \end{pmatrix},$$

where
$V_1 = r_1 - 2C^*r_1 - aN^* - bI^*, V_2 = aC^*, V_3 = bC^*, V_4 = -dN^*, V_5 = r_2 - 2r_2N^* - dC^*, V_6 = -gI^*, V_7 = gC^* + h$ and $M_1 = \frac{efI^*}{(C^*+f)^2}, M_2 = \frac{eC^*}{(C^*+f)}$.
Now the Jacobian matrix of the delayed model (5.1) around the equilibrium point $E^*(C^*, N^*, I^*)$ is

$$J_{E^*} = \begin{pmatrix} V_1 - \lambda & -V_2 & -V_3 \\ V_4 & V_5 - \lambda & 0 \\ V_6 + M_1e^{-\lambda\tau} & 0 & M_2e^{-\lambda\tau} - V_7 - \lambda \end{pmatrix}.$$

Then the characteristic equation of the delay system (5.1) at the

equilibrium point $E^*(C^*, N^*, I^*)$ is

$$\lambda^3 + P_1\lambda^2 + P_2\lambda + P_3 = e^{-\lambda\tau}[\lambda^2 D_1 + \lambda D_2 + D_3], \quad (5.4)$$

where
$P_1 = (V_7 - V_1 - V_5), P_2 = V_1V_5 - V_1V_7 - V_5V_7 - V_2V_4 - V_3V_6, P_3 = V_1V_5V_7 + V_2V_4V_7 - V_3V_5V_6, D_1 = M_2, D_2 = -M_2(V_1 + V_5) - M_1V_3, D_2 = M_2(V_1V_5 + V_2V_4) - M_1V_3V_5$.

5.1.2. Local stability and Hopf-bifurcation

The coexisting equilibrium point E^* will be locally asymptotically stable if all the roots of the corresponding characteristic equation (5.3) are negative or having negative real parts. The classical Routh-Hurwitz criterion can not be used to investigate the stability of the system.

Let $\lambda(\tau) = \alpha(\tau) + i\omega(\tau)$ be the eigenvalue of the characteristic equation (5.3), substituting this value in equation (5.4), we obtain real and imaginary part respectively as

$$\alpha^3 - 3\alpha\omega^2 + P_1(\alpha^2 - \omega^2) + P_2\alpha + P_3 = e^{-\alpha\tau}[\{D_1(\alpha^2 - \omega^2) + D_2\alpha + D_3\}\cos\omega\tau + (2D_1\alpha\omega + \omega D_2)\sin\omega\tau] \quad (5.5)$$

and

$$3\alpha^2\omega - \omega^3 + 2P_1\alpha\omega + P_2\omega = e^{-\alpha\tau}[(2D_1\alpha\omega + D_2\omega)\cos\omega\tau - \{(\alpha^2 - \omega^2)D_1 + \alpha D_2 + D_3\}\sin\omega\tau]. \quad (5.6)$$

A necessary condition for a change in the stability of the equilibrium point E^* is that the corresponding characteristic equation (5.4) admits purely imaginary roots. To examine this condition, we set α=0 in equations (5.5) and (5.6), which leads to the following results:

$$P_3 - P_1\omega^2 = (-D_1\omega^2 + D_3)\cos\omega\tau + D_2\omega\sin\omega\tau, \quad (5.7)$$

and

$$P_2\omega - \omega^3 = D_2\omega\cos\omega\tau - (-D_1\omega^2 + D_3)\sin\omega\tau. \quad (5.8)$$

Eliminating τ by squaring and adding (5.7) and (5.8), we obtain the following equation for determining ω as

$$\omega^6 + (P_1^2 - 2P_2 - D_1^2)\omega^4 + (P_2^2 - 2P_1P_3 - D_2^2 + 2D_1D_3)\omega^2 + (P_3^2 - D_3^2) = 0. \quad (5.9)$$

Using substitution of $\omega^2 = \zeta$ in the equation (5.9), we reduce it to the following cubic equation:

$$k(\zeta) = \zeta^3 + \sigma_1\zeta^2 + \sigma_2\zeta + \sigma_3 = 0, \quad (5.10)$$

where $\sigma_1 = P_1^2 - 2P_2, \sigma_2 = P_2^2 - 2P_1P_3 - D_1^2, \sigma_3 = P_3^2 - D_2^2$.

Now, if the coefficients σ_1 and σ_3 have opposite sign then by *Descarte's rule of sign* equation (5.10) has at least one positive root for either sign of σ_2. The following theorem establishes a criterion for determining changes in the stability of the equilibrium point E^* with respect to the delay parameter τ.

Theorem 5.1 *Suppose that the interior equilibrium point E^* exists and locally asymptotically stable for τ=0. Also let $\zeta_0 = \omega_0^2$ ba a positive root of (5.10).*

(1) Then $\exists\ \tau = \tau^*$ such that the interior equilibrium point E^* of the delay system (5.1) is asymptotically stable when $0 \le \tau < \tau^*$ and unstable for $\tau > \tau^*$.
(2) Furthermore, the system will undergo a Hopf-bifurcation at E^* when $\tau = \tau^*$, provided $W(\omega)X(\omega) - Z(\omega)Y(\omega)) > 0$.

Proof: As ω_0 is a solution of eq.(5.9), then the characteristic eq.(5.4) has purely imaginary roots $\pm i\omega_0$. From the equations (5.7) and (5.8), we have ${\tau_n}^*$ is a function of w_0 for $n = 0, 1, 2, ...$; which is given by

$${\tau_n}^* = \frac{1}{\omega_0}\arccos\left[\frac{(P_1D_1 - D_2)\omega_0^4 + P_D\omega_0^2 + P_3D_3}{(D_2\omega_0)^2 + (D_3 - D_1\omega_0^2)^2}\right] + \frac{2\pi p}{\omega_0}, \quad \text{where } P_D = P_2D_2 - P_1D_3 - P_3D_1. \quad (5.11)$$

The system will be locally asymptotically stable around the interior equilibrium point E^* for $\tau = 0$ if the condition $\sigma_1\sigma_2 - \sigma_3 > 0$. In this case by Butler's lemma, E^* will remain stable for $\tau < \tau^*$ such that $\tau^* = \min_{m\ge 0} {\tau_n}^*$ and E^* will be unstable for $\tau \ge \tau^*$, when the transversality condition holds.

Transversality condition:

We now proceed to verify the transversality condition,
$\frac{d}{d\tau}[Re(\lambda(\tau))]_{\tau=\tau^*} > 0$.
Now differentiating eq. (5.4) with respect to τ and then putting $\alpha = 0$ we get ,
$\frac{d\alpha}{d\tau}[-3\omega^2 + P_2 + \tau\{cos\omega\tau(-\omega^2D_1 + D_3) + \omega D_2 sin\omega\tau\} - D_2 cos\omega\tau - 2\omega D_1 sin\omega\tau] + \frac{d\omega}{d\tau}[-2\omega P_1 + \tau sin\omega\tau(-\omega^2D_1 + D_3) + 2\omega D_1 cos\omega\tau - D_2 sin\omega\tau - \tau\omega D_2 cos\omega\tau] = -\omega(-\omega^2D_1 + D_3)sin\omega\tau + \omega^2 D_2 cos\omega\tau$.
Differentiating eq. (5.5) with respect to τ and putting α=0 then we get ,
$-\frac{d\alpha}{d\tau}[-2\omega P_1 + \tau sin\omega\tau(-\omega^2D_1 + D_3) + 2\omega D_1 cos\omega\tau - D_2 sin\omega\tau - \tau\omega D_2 cos\omega\tau] + \frac{d\omega}{d\tau}[-3\omega^2 + P_2 + \tau\{cos\omega\tau(-\omega^2D_1 + D_3) + \omega D_2 sin\omega\tau\} - D_2 cos\omega\tau - 2\omega D_1 sin\omega\tau] = -\omega^2 D_2 sin\omega\tau - \omega cos\omega\tau(-\omega^2D_1 + D_3)$.
We can rewrite the above two equations as

$$X(\omega)\frac{d\alpha}{d\tau} + Y(\omega)\frac{d\omega}{d\tau} = W(\omega) \quad (5.12)$$

and

$$-Y(\omega)\frac{d\alpha}{d\tau} + X(\omega)\frac{d\omega}{d\tau} = Z(\omega) \quad (5.13)$$

where
$X(\omega) = -3\omega^2 + P_2 + \tau\{cos\omega\tau(-\omega^2D_1 + D_3) + \omega D_2 sin\omega\tau\} - D_2 cos\omega\tau - 2\omega D_1 sin\omega\tau$,
$Y(\omega) = -2\omega P_1 + \tau sin\omega\tau(-\omega^2D_1 + D_3) + 2\omega D_1 cos\omega\tau - D_2 sin\omega\tau - \tau\omega D_2 cos\omega\tau$,
$W(\omega) = -\omega(-\omega^2D_1 + D_3)sin\omega\tau + \omega^2 D_2 cos\omega\tau$,
$Z(\omega) = -\omega^2 D_2 sin\omega\tau - \omega cos\omega\tau(-\omega^2D_1 + D_3)$.
From (5.12) and (5.13) we have ,
$\frac{d}{d\tau}[Re(\lambda(\tau))]_{\tau=\tau^*,\ \omega=\omega_0} = \frac{W(\omega)X(\omega) - Z(\omega)Y(\omega))}{X^2(\omega) + Y^2(\omega)}$,
which shows that
$\frac{d}{d\tau}[Re(\lambda(\tau))]_{\tau=\tau^*,\ \omega=\omega_0} > 0$ if $W(\omega)X(\omega) - Z(\omega)Y(\omega)) > 0$.
Therefore, the transversality condition is satisfied and hence Hopf bifurcation occurs at $\tau = \tau^*$. This completes the proof of the theorem.

6. Numerical simulations

6.1. Numerical simulations without delay

In this section, we present numerical simulations of system (2.1) to validate the earlier analytical results. All simulations are carried out using MATLAB. This study highlights system stability, bifurcation phenomena, limit-cycle formation, higher-order periodic oscillations, and chaotic dynamics.

For illustrative purpose, we use the following parameter values:

$$a = 1, b = 2.5, d = 1.5, e = 2.4, f = 1, g = 0.2, \\ h = 0.5, p = 0.5, r_1 = 1, r_2 = 0.6, \tag{6.1}$$

and we choose the initial condition as $[C(0), N(0), I(0)] = [0.3, 0.7, 0.2]$.

Our investigation begins by the examining the dynamical behaviors of the system (2.1) as we vary the maximum growth rate of effector cells, denoted by e. Increasing the growth rate of effector cells in the presence of cancer cells leads to the system to move from stable focus to chaotic oscillation behaviors. At $e = 2.4$, the system demostrates a stable solution (see Fig. 1).

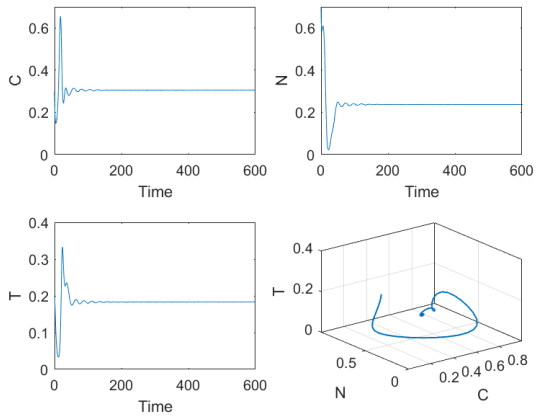

Figure 1. The first row left figure is the time series for the cancer cells; the first row right figure is the time series for the normal cells; the second row left figure is the time series for the immune cells and the second row right figure is the 3D phase portrait of the stable interior equilibrium of the system (2.1). Here $e = 2.5$ and the other parameters remained same as in (6.2) and the inital condition is $[C(0), N(0), I(0)] = [0.3, 0.7, 0.2]$.

The system displays limit cycle oscillation at $e = 2.8$ (see Figure 2). However at $e = 3.4$ and $e = 4.5$ the system shows 2-periodic oscillations (see Figure 3) and chaotic dynamics (see Figure 4) respectively.

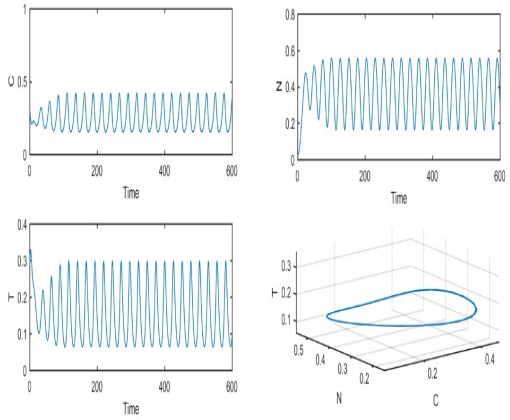

Figure 2. This figure illustrates that system (2.1) exhibits limit cycle oscillation when $e = 2.8$ and the other parameter values kept same as in Figure 1.

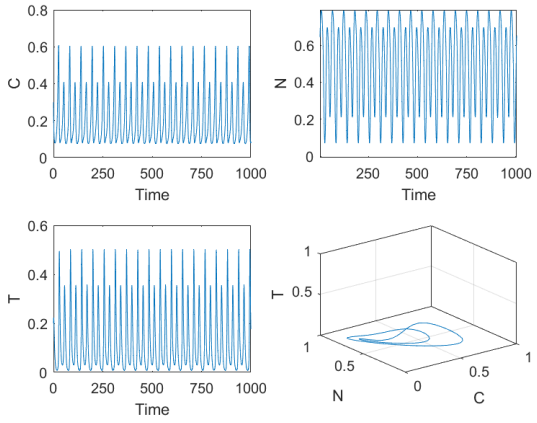

Figure 3. This figure represents that system (2.1) shows two-periodic oscillation when $e = 3.4$ and the other parameter values kept unaltered as in Figure 1.

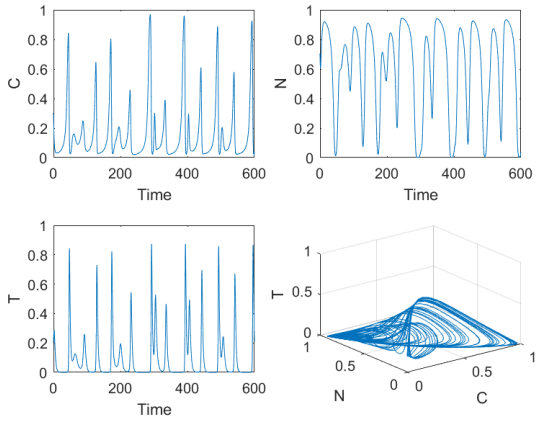

Figure 4. This figure represents that the system (2.1) becomes chaotic for $e = 4.5$ and the other parameter values kept same as in Figure 1.

From the above figures, we observe that as the proliferation rate of immune cells in the presence of cancer cells is gradually increased, the system enters a chaotic regime via a period-doubling bifurcation. Biologically, increasing e corresponds to stronger immune activation or proliferation, which may arise from immunotherapy, enhanced antigen presentation, or increased immune sensitivity to tumor signals. While moderate immune stimulation stabilizes tumor–immune interactions, excessive immune proliferation introduces strong nonlinear feedback, leading to repeated cycles of immune overactivation and tumor suppression followed by immune decline and tumor regrowth. These oscillatory cycles undergo successive period-doubling bifurcations and eventually transition to chaotic dynamics, reflecting a loss of immune regulation. Such chaotic behavior represents unpredictable tumor–immune interactions and may help explain irregular tumor growth, immune escape, and variable treatment responses observed during cancer progression.

6.2. Numerical simulations with delay

In this section, we conduct numerical simulations of system (5.1) for different values of τ. Here we have chosen the same parameter

values i.e.

$$a = 1, b = 2.5, d = 1.5, e = 2.4, f = 1, g = 0.2, h = 0.5, \\ p = 0.5, r_1 = 1, r_2 = 0.6. \tag{6.2}$$

In the absence of delay (i.e. $\tau = 0$), the system (5.1) shows stable of all cells at the equilibrium point $E^*(0.3051, 0.2373, 0.1830)$ while the parameter values are same as above.

To investigate the impact of activation delay in the immune response, we gradually increase the value of the delay parameter τ. We observe that the system remains stable for very small time delays, for example at $\tau = 0.05$ (see Figure 5).

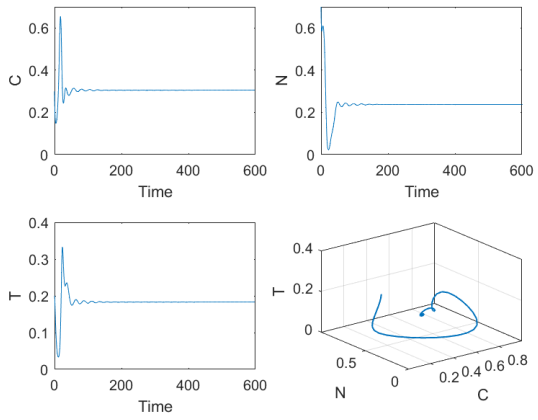

Figure 5. This figure represents that the system (5.1) is stable for $\tau = 0.05$ and the other parameter values kept same as in equation (6.2).

Now, as the value of τ is increased, system (5.1) undergoes a Hopf bifurcation when the delay parameter τ crosses its critical value $\tau_0 = 0.06$. Consequently, the system loses stability and gives rise to limit-cycle oscillations. For $\tau = 1$, system (5.1) exhibits sustained limit-cycle oscillations (see Figure 6).

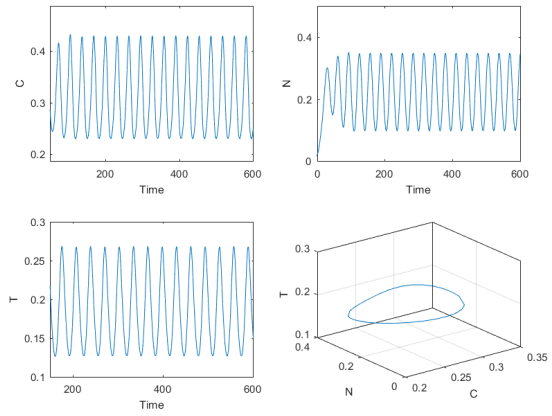

Figure 6. This figure represents that the system (5.1) shows limit cycle oscillation for $\tau = 1$, while other parameter values kept same as in equation (6.2).

With a further increase in the time delay, the system (5.1) exhibits period-doubling behavior. At $\tau = 2$, the system shows 2-periodic limit-cycle oscillations (see Figure 7). For $\tau = 2.1$, the system exhibits 4-periodic limit-cycle oscillations (see Figure 8). Higher-order periodic oscillations and chaotic dynamics are observed as the time delay is increased further. In particular, for $\tau = 2.2$, system (5.1) enters a chaotic regime (see Figure 9).

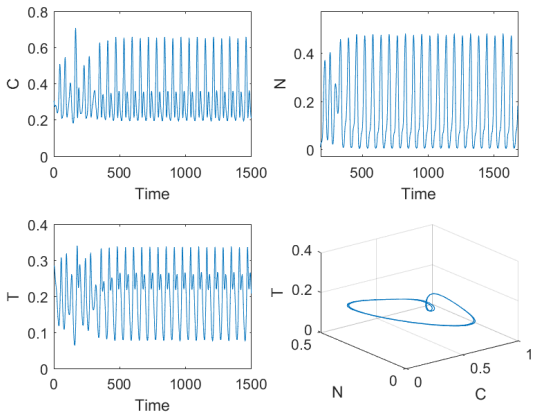

Figure 7. This figure represents that the system (5.1) shows 2-periodic oscillation for $\tau = 2$ and the other parameter values kept same as in equation (6.2).

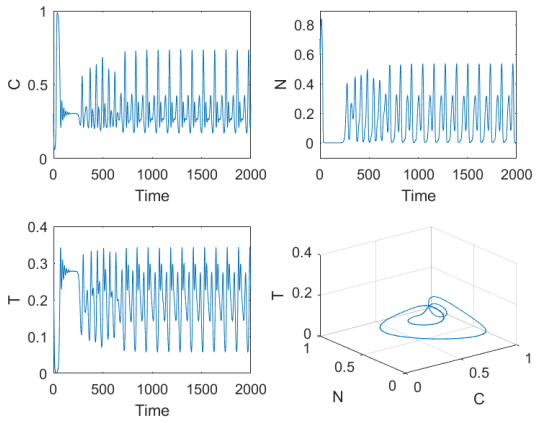

Figure 8. This figure represents that the system (5.1) shows 4-periodic oscillation for $\tau = 2.1$ and the other parameter values kept same as in equation (6.2).

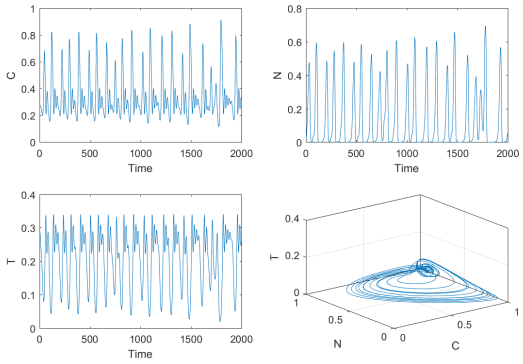

Figure 9. This figure represents that the system (5.1) becomes chaotic for $\tau = 2.2$ and the other parameter values kept same as in equation (6.2).

For better visualization, we construct the bifurcation diagram of system (5.1) (Figure 10), taking τ as the bifurcation parameter. We observe that the system remains stable for $0 \leq \tau < 0.06$. Limit-cycle oscillations occur for $0.06 \leq \tau \leq 1.2$. The system undergoes period-doubling bifurcations for $1.2 < \tau \leq 2.1$. Finally, for $\tau > 2.1$, the system exhibits higher-order periodic oscillations and chaotic dynamics.

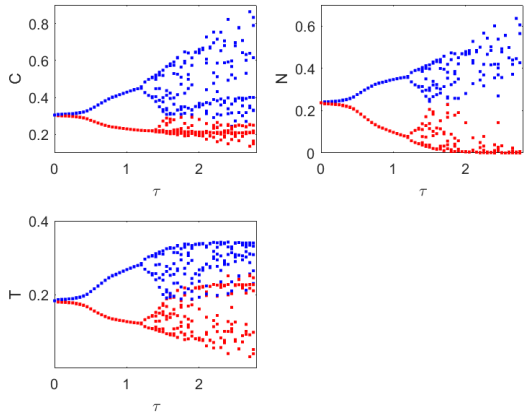

Figure 10. Bifurcation diagrams with respect to τ for system (5.1), where the other parameters are remained same as in Figure 1.

In system (5.1), the delay parameter τ represents the finite time required for immune cells to become activated and proliferate in response to cancer cells. Biologically, this delay may arise from processes such as antigen recognition, immune cell differentiation, clonal expansion, and intracellular signaling cascades. In the absence of delay ($\tau = 0$), the immune response is effectively instantaneous, allowing the system to maintain a stable focus through efficient feedback regulation. In contrast, increasing the delay τ introduces memory effects into the immune response, causing immune cells to react to past tumor levels rather than the current state. This delayed feedback destabilizes the equilibrium, leading to oscillatory behavior, period-doubling bifurcations, and ultimately chaotic dynamics. Biologically, such chaos reflects a loss of synchronization between tumor growth and immune activation, resulting in irregular tumor control and unpredictable disease progression.

7. Conclusion

Mathematical oncology is an emerging research area in which mathematical models are developed to describe and quantitatively relate the key physical and biological factors that influence cancer development, invasion, metastasis, treatment response, and therapeutic resistance. At the individual level, mathematical modeling has been employed to understand the mechanisms by which the immune system combats cellular diseases and to propose potential intervention strategies. At a broader level, mathematical biologists have developed theoretical frameworks to analyze, predict, and control cancer progression and spread.

In the present study, we investigate the global dynamics of a cancer model that captures the interactions among cancer cells, normal cells, and immune effector cells activated in response to the presence of cancer. For lower values of the immune effector cell activation rate (e), the immune response is moderate and well regulated, allowing cancer cells and normal cells to coexist around a biologically feasible interior equilibrium. As the activation rate (e) increases, representing enhanced immune stimulation, the intensified immune–tumor interaction destabilizes the steady state, leading first to sustained oscillations in the population densities. Further increase in (e) results in complex dynamical behavior, with the system ultimately entering a chaotic regime, reflecting irregular and unpredictable immune-mediated tumor control.

In the second scenario, a time delay is incorporated into the system to account for the finite time required for immune cells to become activated and proliferate in response to cancer cells. The introduction of this delay significantly enriches the system dynamics. For small delays, the immune response remains timely and effective, allowing the system to maintain stability. As the delay increases, the misalignment between tumor growth and immune activation leads to limit-cycle oscillations, followed by two-periodic oscillations. Further increases in the delay result in four-periodic oscillations and eventually give rise to higher-order periodic and chaotic dynamics, reflecting irregular and unpredictable tumor control by the immune system.

In conclusion, our study demonstrates that both the immune effector cell activation rate and the activation delay critically influence tumor–immune dynamics. Moderate immune responses maintain system stability, whereas increased activation or longer delays can induce oscillations and chaotic behavior, highlighting the complex and sensitive nature of immune-mediated tumor control.

In summary, our study demonstrates that both the immune effector cell activation rate and the activation delay play critical roles in shaping tumor–immune dynamics. Moderate immune responses help maintain system stability, whereas increased activation or longer delays can induce oscillatory and chaotic behavior, highlighting the complex and sensitive nature of immune-mediated tumor control.

8. ACKNOWLEDGEMENTS

The authors are thankful to the learned Editor and the reviewers for their constructive comments and valuable suggestions, which have significantly helped to improve the quality of the manuscript. One of the authors (Riya Kundu) acknowledges financial support provided by UGC through the award of a Junior Research Fellowship (NTA Ref. No.: 211610106562).

REFERENCES

[1] Ann F Chambers, Alan C Groom, and Ian C MacDonald. Dissemination and growth of cancer cells in metastatic sites. *Nature Reviews Cancer*, 2(8):563–572, 2002.

[2] Lindsey A Torre, Freddie Bray, Rebecca L Siegel, Jacques Ferlay, Joannie Lortet-Tieulent, and Ahmedin Jemal. Global cancer statistics, 2012. *CA: a Cancer Journal for Clinicians*, 65(2):87–108, 2015.

[3] William B Coley. The classic: The treatment of malignant tumors by repeated inoculations of erysipelas: With a report of ten original cases. *Clinical Orthopaedics and Related Research®*, 262:3–11, 1991.

[4] Baruch S Blumberg. Hepatitis b virus, the vaccine, and the control of primary cancer of the liver. *Proceedings of the National Academy of Sciences*, 94(14):7121–7125, 1997.

[5] Linda J Rogers, Lois J Eva, and David Michael Luesley. Vaccines against cervical cancer. *Current Opinion in Oncology*, 20(5):570–574, 2008.

[6] Judah Folkman et al. Tumor angiogenesis: therapeutic implications. *The New England Journal of Medicine*, 285 (21):1182–1186, 1971.

[7] Herbert Hurwitz, Louis Fehrenbacher, William Novotny, Thomas Cartwright, John Hainsworth, William Heim, Jordan Berlin, Ari Baron, Susan Griffing, Eric Holmgren, et al. Bevacizumab plus irinotecan, fluorouracil, and leucovorin for metastatic colorectal cancer. *New England Journal of Medicine*, 350(23):2335–2342, 2004.

[8] Bruce J Giantonio, Paul J Catalano, Neal J Meropol, Peter J O'Dwyer, Edith P Mitchell, Steven R Alberts, Michael A Schwartz, and Al B Benson III. Bevacizumab in combination with oxaliplatin, fluorouracil, and leucovorin (folfox4) for previously treated metastatic colorectal cancer: results from the eastern cooperative oncology group study e3200. *Journal of Clinical Oncology*, 25(12):1539–1544, 2007.

[9] Alan Sandler, Robert Gray, Michael C Perry, Julie Brahmer, Joan H Schiller, Afshin Dowlati, Rogerio Lilenbaum, and David H Johnson. Paclitaxel–carboplatin alone or with bevacizumab for non–small-cell lung cancer. *New England Journal of Medicine*, 355(24):2542–2550, 2006.

[10] Philip Hahnfeldt, Dipak Panigrahy, Judah Folkman, and Lynn Hlatky. Tumor development under angiogenic signaling: a dynamical theory of tumor growth, treatment response, and postvascular dormancy. *Cancer Research*, 59 (19):4770–4775, 1999.

[11] Ayla Ergun, Kevin Camphausen, and Lawrence M Wein. Optimal scheduling of radiotherapy and angiogenic inhibitors. *Bulletin of Mathematical Biology*, 65(3):407–424, 2003.

[12] Alberto d'Onofrio and Alberto Gandolfi. Tumour eradication by antiangiogenic therapy: analysis and extensions of the model by hahnfeldt et al.(1999). *Mathematical biosciences*, 191(2):159–184, 2004.

[13] Hoang Pham. Mathematical modeling the time-delay interactions between tumor viruses and the immune system with the effects of chemotherapy and autoimmune diseases. *Mathematics*, 10(5):756, 2022.

[14] Norman MacDonald. *Time lags in biological models*, volume 27. Springer Science & Business Media, 2013.

[15] Yang Kuang. *Delay differential equations: with applications in population dynamics*, volume 191. Academic press, 1993.

[16] David Greenhalgh, Sourav Rana, Sudip Samanta, Tridip Sardar, Sabyasachi Bhattacharya, and Joydev Chattopadhyay. Awareness programs control infectious disease–multiple delay induced mathematical model. *Applied Mathematics and Computation*, 251:539–563, 2015.

[17] Santanu Biswas, Md Saifuddin, Sourav Kumar Sasmal, Sudip Samanta, Nikhil Pal, Faisal Ababneh, and Joydev Chattopadhyay. A delayed prey–predator system with prey subject to the strong allee effect and disease. *Nonlinear Dynamics*, 84(3):1569–1594, 2016.

[18] Nikhil Pal, Sudip Samanta, Santanu Biswas, Marwan Alquran, Kamel Al-Khaled, and Joydev Chattopadhyay. Stability and bifurcation analysis of a three-species food chain model with delay. *International Journal of Bifurcation and Chaos*, 25(09):1550123, 2015.

[19] Santanu Biswas, Sourav Kumar Sasmal, Sudip Samanta, Md Saifuddin, Qamar Jalil Ahmed Khan, and Joydev Chattopadhyay. A delayed eco-epidemiological system with infected prey and predator subject to the weak allee effect. *Mathematical Biosciences*, 263:198–208, 2015.

[20] Sudip Samanta, Pankaj Kumar Tiwari, Abdullah K Alzahrani, and Ali Saleh Alshomrani. Chaos in a nonautonomous eco-epidemiological model with delay. *Applied Mathematical Modelling*, 79:865–880, 2020.

[21] Kakali Ghosh, Santanu Biswas, Sudip Samanta, Pankaj Kumar Tiwari, Ali Saleh Alshomrani, and Joydev Chattopadhyay. Effect of multiple delays in an eco-epidemiological model with strong allee effect. *International Journal of Bifurcation and Chaos*, 27(11):1750167, 2017.

[22] Sudip Samanta. Controlling population oscillations in a delayed lotka-volterra model with z-type control. *Mathematics in Engineering, Science & Aerospace (MESA)*, 16(1), 2025.

[23] Edoardo Beretta and Yoshiko Takeuchi. Global stability of single-species diffusion volterra models with continuous time delays. *Bulletin of Mathematical Biology*, 49(4):431–448, 1987.

[24] Edoardo Beretta, Margherita Carletti, Denise E Kirschner, and Simeone Marino. Stability analysis of a mathematical model of the immune response with delays. In *Mathematics for Life Science and Medicine*, pages 177–206. Springer, 2006.

[25] Shigui Ruan. Delay differential equations in single species dynamics. In *Delay differential equations and applications*, pages 477–517. Springer, 2006.

[26] Lifeng Han, Changhan He, and Yang Kuang. Dynamics of a model of tumor-immune interaction with time delay and noise. *Discrete Contin. Dyn. Syst. Ser. S*, 13:2347–2363, 2020.

[27] Subhas Khajanchi, Matjaž Perc, and Dibakar Ghosh. The influence of time delay in a chaotic cancer model. *Chaos: An Interdisciplinary Journal of Nonlinear Science*, 28(10), 2018.

[28] Subhas Khajanchi. Chaotic dynamics of a delayed tumor–immune interaction model. *International Journal of Biomathematics*, 13(02):2050009, 2020.

[29] Magda Galach. Dynamics of the tumor-immune system competition-the effect of time delay. *International Journal of Applied Mathematics and Computer Science*, 13(3):395–406, 2003.

[30] Vladimir A Kuznetsov, Iliya A Makalkin, Mark A Taylor, and Alan S Perelson. Nonlinear dynamics of immunogenic tumors: parameter estimation and global bifurcation analysis. *Bulletin of Mathematical Biology*, 56(2):295–321, 1994.

[31] WHO. Cancer, 2025. URL https://www.who.int/health-topics/cancer.

[32] G Birkhoff and GC Rota. *Ordinary Differential Equations, Ginn, Boston*. John Wiley & Sons Inc, 1982.

[33] Jack K Hale. Functional differential equations. In *Analytic Theory of Differential Equations: The Proceedings of the Conference at Western Michigan University, Kalamazoo, from 30 April to 2 May 1970*, pages 9–22. Springer, 2006.